Aging of oil-impregnated paper at different frequencies

Niasar, Mohamad Ghaffarian; Zhao, Weichuan

DOI
10.1109/ICPADM49635.2021.9493911

Publication date
2021

Document Version
Accepted author manuscript

Published in
13th International Conference on the Properties and Applications of Dielectric Materials

Aging of oil-impregnated paper at different frequencies

Mohamad Ghaffarian Niasar
Electrical Sustainable Energy
Delft University of Technology
Delft, Netherlands
M.GhaffarianNiasar@tudelft.nl

Weichuan Zhao
Electrical Sustainable Energy
Delft University of Technology
Delft, Netherlands
W.Zhao-3@tudelft.nl

***Abstract*—In this work, breakdown strength and lifetime curve of oil-impregnated paper (OIP) are compared at 50Hz and 1500 Hz. For the ramp breakdown tests, sinusoidal voltage ramp of 1 kV_p/s is used. The ramp breakdown experiments is conducted on OIP samples made of single and double sheets of OIP. Weibull plots and interpretation of the results are presented. In order to obtain lifetime curves, a step sinusoidal voltage waveform whose peak value is close to the minimum OIP ramp breakdown voltage is applied on single sheet of OIP samples. Time to breakdown is measured, and each experiment is repeated between 20-30 times to obtain good statistical results. The experiments were focused on four different voltage levels and the lifetime curves are plotted for those two target frequencies. Parameters of the lifetime curves are extracted and the interpretation is given.**

Keywords—Oil-impregnated paper, lifetime curve, aging, breakdown voltage, high frequency electric stress

I. INTRODUCTION

Flexible voltage and power flow control are two of the important features of the future smart grid, which cannot be fully achieved through conventional transformer and mechanical tap changers. During the past two decades, highly controllable solid state transformer (SST) has been under development to fill this gap. A critical component inside SST is the medium frequency transformer (MFT) by which galvanic isolation is provided between the primary and secondary sides of SST. High voltage (>10kV) SiC semiconductor switches with reasonable current capabilities will be introduced to the market in the coming years. By means of such switches, the construction of SST using cascaded H-bridge (CHB) or modular multilevel converters (MMC) topology, will be simplified since lower number of sub-modules are necessary to handle the medium voltage. However, due to the presence of very high dv/dt, different challenges need to be addressed, one of which is the degradation of insulation material under such electric stress.

To have a reliable SST with long lifetime, the insulation system of MFT must withstand high frequency high voltage stress over its life period. To design a reliable insulation system for MFT, lifetime curves of insulation material under different frequencies must be obtained first. From lifetime curves, the desired converter lifetime, and operating condition of the converter (voltage waveform on transformer winding may differ depending on the converter topology), permissible electric field can be identified and also, proper thickness of insulation material as well as sufficient electric field grading needed for the design of MFT, can be selected. While the breakdown and lifetime curve of different insulation material have been widely investigated for 50 Hz AC, the impact of frequency and voltage waveform on insulation degradation are not conclusive. Significant amount of work has been done on machine winding insulation [1-6].

In general, it is concluded that when partial discharge exists, the lifetime decreases with the increase of switching frequency (lifetime $\propto f^{-k}$). Factor k is obtained to be 1 according to [1] and less than 1 (typically between 0.6-0.8) according to [2]. Faster rise time of the voltage pulses, in case PD is present, results in lower lifetime and higher amplitude of PD [3, 4]. In general when PD exists, the lifetime increases if the duty cycle of the applied voltage decreases [5, 6]. When PD does not exist, there are number of factors that impact the lifetime, such as peak and rms value of the voltage waveform, frequency, temperature, harmonics content, etc. Cavallani, et. al. [7] proposed (1) that relates the lifetime to the voltage peak, voltage rms and harmonics content. According to experimental results, peak voltage has the most significant impact on insulation lifetime.

$$L = L_0 {K_p}^{-n_p} {K_{rms}}^{-n_{rms}} {K_s}^{-n_s} \quad (1)$$

Higher frequencies or harmonics content, result in extra dielectric loss which may lead to overheating [3, 8, 9]. Comparison of impact of over temperature and peak-to-peak value of voltage are presented in [7]. The results show that temperature has less impact compared to the impact of peak-to-peak of applied voltage. The lifetime decreases with the increase of frequency [10] and slew rate. Reference [11] proposed (2) which relates lifetime and frequency.

$$L_f = L_1 \left(\frac{f_1}{f}\right)^{\gamma} \quad (2)$$

Various types of insulation material such as paper insulation, epoxy resin, polyamide film, polypropylene and etc. [12] are the potential candidates for the insulation system of MFT. For high voltage MFT, the design of insulation system using dry type insulation material would be very difficult. An alternative solution is the liquid immersed MFT. Properties of oil-impregnated paper (OIP) insulation system have been investigated thoroughly at 50 Hz and DC in available literature [13]. In this paper, the breakdown strength and lifetime of OIP are studied and compared at 50 Hz and 1500 Hz. The Lifetime curves of OIP are plotted and the obtained parameters of the curves (slope and y-intercept) are compared between two target frequencies.

II. SAMPLE PREPARATION AND EXPERIMENTAL SETUP

A. OIP sample preparation

In this study, mineral oil, type Nynas Nytro Taurus is used as the impregnating medium. The paper used is Tervakovski cable paper with an average thickness of 0.15 mm. The paper samples were impregnated inside a BINDER VD 53 vacuum oven. A large paper sheet was first cut into small circular

pieces suitable for the test set-up. The impregnation procedure is as follow:

1- Paper samples were vacuum dried at 120 °C for 24 h

2- Oven temperature was reduced gradually to 60 °C, the chamber was filled with dry nitrogen and oil container was placed into the chamber. Vacuum pump was turned on and the pressure of chamber was lowered to 5 mbar and kept at that level. Both oil and paper samples were vacuum dried (5 mbar) at 60 °C for another 24 hours

3- The chamber was filled with dry nitrogen and the paper samples were placed inside oil container. The paper samples were impregnated under vacuum at 60 °C for 24 hours.

4- The heater was turned off and oil paper samples were left inside vacuum chamber to cool down.

After the impregnation processes, the OIP samples were always kept below the oil level inside a sealed desiccator to limit moisture ingress. Prior to each experiment, required number of samples together with sufficient amount of oil were transferred to another glass container from which the samples were taken and placed between the electrodes of the test setup. Fig. 1 shows the samples at different stages of sample preparation.

Fig. 1. Sample preparation. Paper roll, small circular paper samples, OIP samples stored inside a closed desiccator, OIP samples transferred to another glass container to be used for the test.

B. *Experimental set-up*

A 30 kV Trek amplifier is used to generate high voltage at different frequencies. The Trek amplifier is equipped with an internal voltage divider which is used to measure its output voltage. The input signal is produced by a TENUMA 72-14111 function generator. The electrodes are made of stainless steel with a diameter of 40 mm and rounded edges of 3 mm radius. The support structure is made of Teflon and is held together by Nylon screws and bolts. Fig. 2 shows the experimental set-up.

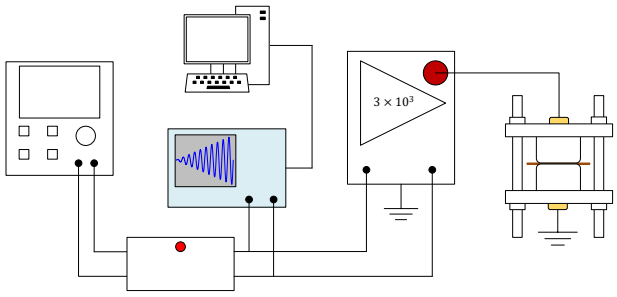

Fig. 2. Experimental setup used to perform breakdown and lifetime tests

Even though the Trek amplifier has its in-built fault detection circuitry, due to the small thickness of the OIP samples, in many cases amplifier fault detection mechanism takes many cycles to operate especially at higher frequencies. This would cause the formation of carbonized spots on the surface of electrodes after each experiment which may change the electric field at those positions for the next experiments. These spots can be removed by polishing the electrodes. To minimize this effect, a control box is added between the function generator and the amplifier. The output voltage measured by the amplifier is fed back to this control box and as soon as voltage drops below a threshold over a pre-defined time period, this control box stops the input signal to the amplifier. The control box is made with an Arduino microcontroller and is capable of detection of breakdown within a few cycles at different frequencies, which is much faster than in-built fault detection system of the amplifier. Using this approach, discharge spots were almost eliminated. Therefore, the electrodes were polished only after each set of experiments rather than after each individual experiment.

For the ramp sinusoidal breakdown tests, sine waveform was modulated with a ramp signal in the function generator. The function generator produced continuous ramp sinusoidal waveform. In order to force the ramp breakdown test to start exactly at the beginning of a ramp, the synchronization signal of the function generator is fed to the control box. When a user pushes the button on the control box, microcontroller detects the beginning of the next ramp by means of the synchronization signal, a relay inside the control box is activated and the output of function generator is connected to the amplifier. In this way, it was ensured that all ramp sinusoidal breakdown tests were started from the beginning of a ramp and increased with an exact 1 kV_p/s rate.

III. RAMP SINUSOIDAL BREAKDOWN TEST

The ramp breakdown experiments were performed on OIP samples made of one or two sheets of OIP. A ramp sinusoidal voltage with slope of 1 kV_p/s is applied to the electrodes, once at 50 Hz and once at 1500 Hz. To have a good statistics, at least 30 experiments were performed for each case study. After each experiment, the thickness of OIP sample was measured at the point of breakdown. The scatter of the thickness data is shown in Fig. 3. Breakdown strength is measured by dividing the applied voltage to the corresponding sample thickness at the point of breakdown. It is important to notice that since here we have a two phase system (oil and paper), and because oil has also high breakdown strength, in many cases the point of breakdown has even higher thickness compared with other parts of the sample under electrodes.

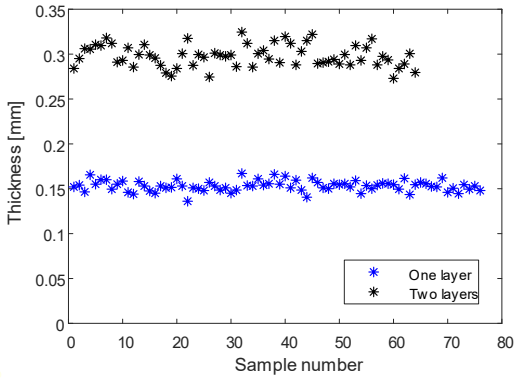

Fig. 3. Variation of sample thickness

2-parameter Weibull distribution shown in (3) is used to analyse the data.

$$F(E) = 1 - e^{-\left(\frac{E}{\eta}\right)^{\beta}} \quad (3)$$

In (3), E is breakdown strength, F(E) is the cumulative probability of breakdown, β is the shape parameter which reflects the slope of regression line in the probability plot, and η is the scale parameter. Probability of breakdown for the specimens is 63.2% at an electric field strength equal to η. Furthermore, in Weibull distribution plot there is another important parameter named correlation factor ρ, which is an indicator showing how well the linear regression line fits the data. Weibull plots of ramp sinusoidal breakdown for one and two layers of OIP at 50 Hz and 1500 Hz is shown in Fig. 4. Table I shows a summary of Weibull distribution parameters for the plots shown in Fig.4. A number of important observations can be made.

First of all, the breakdown strength at 50 Hz is considerably higher than that at 1500 Hz (also visible in parameter η shown in table I). The slope of Weibull plot is more at 50 Hz compared with that at 1500 Hz (also visible in parameter β shown in table I). It can be seen that at 50 Hz the spread of breakdown strength is narrower, i.e. within a span of 25 kV/mm (from 65kV/mm-90 kV/mm) all samples undergo breakdown. However, for 1500 Hz, the spread is wider and within a span of 40 kV/mm (from 35kV/mm-75 kV/mm). This means that weaker samples at higher frequencies behave very poorly. This has very important consequence since insulation system is designed such that even the weakest point of dielectric should handle the electric field stress. If the weakest samples has far lower breakdown strength, it means more insulation material is needed to achieve a reliable design.

Secondly, compared with the plots of one-layer breakdown test, it can be seen that for both 50 Hz and 1500 Hz, the slope of the regression lines for two layers become sharper (also visible in parameter β shown in table I). This is because with more OIP layers it is less likely that two weak points on each OIP layer align. As a consequence, the breakdown strength of material becomes less dependent on each individual sample layer and its weak points. Hence the breakdown strength is less spread.

Thirdly, for both 50 Hz and 1500 Hz, it can be seen that samples made of two layers of OIP have in general lower breakdown strength than those with one layer of OIP. This observation can be referred to the so called volume effect which is usually observed in insulation material. According to this effect, thinner and smaller sample of a piece of insulation material has higher breakdown strength than the thicker and larger ones. The effect is attributed to the number of defects in a given volume of insulation sample. The thicker the sample is, the more likely of the presence of defects inside the sample would be. Therefore, it is more likely that breakdown occurs. However, when considering the lower parts of the curves (probability of failure <20%) which belongs to those samples that have severe weak points (breakdown occurs at the lower range of electric field), there is no clear observation of volume effect and if regression lines are considered, actually the opposite effect is observed. This is because when severe weak points are present (which is true for this part of the curve), for one layer sample, the severe weak point directly lead to breakdown of one layer samples. However, for two layer OIP samples, two severe weak points on each layer is unlikely to be right on top of each other. Therefore, for this part of the curve, the breakdown strength of one layer sample is lower than sample with 2 layers (or multi layers in general).

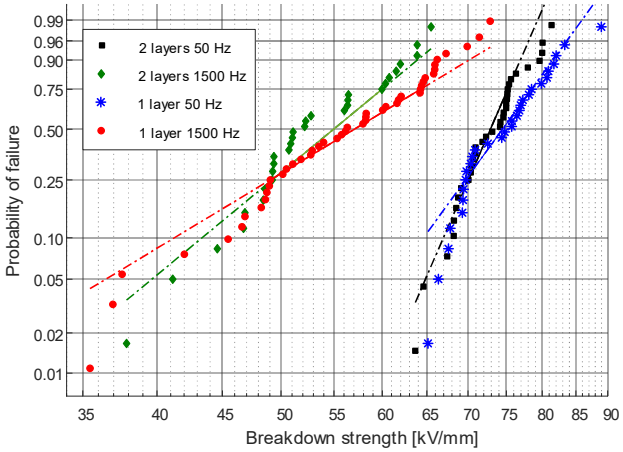

Fig. 4. Comparison of Weibull plots for 1 layer and 2 layers of OIP at 50 Hz and 1500 Hz

TABLE I. WEIBULL DISTRIBUTION PARAMETERS OF PLOTS IN FIG. 4

Parameter	β	$\eta\ (kV_p/mm)$	ρ
One layer 50 Hz	16.85	77.0	0.9468
Two layers 50 Hz	21.28	74.8	0.9750
One layer 1500 Hz	7.29	59.9	0.9907
Two layers 1500 Hz	9.51	56.01	0.9771

IV. LIFETIME TEST

Time to breakdown was measured for 50 Hz and 1500 Hz at different level of electric field stress. At each electric field level, the experiment was repeated at least 21 times (in some cases up to 31 times) to get good statistics. For each electric field strength, the median of the measurements (coloured blue in Fig. 5) was selected to represent the trend of data and to draw the lifetime curve. By fitting the medians into the well-known empirical inverse power low, (4), the lifetime curve can be obtained. Fig. 5. Shows time to breakdown measurement data and the fitted lifetime curves at 50 Hz and 1500 Hz.

$$t = k\left(\frac{E}{E_0}\right)^{-n} \quad (4)$$

In equation 4, t represents for the time, k is a constant and has the unit of time, E is the electric field in $\frac{kV}{mm}$ and E_0 is a constant with the unit of electric field, equal to $1\frac{V}{mm}$. E_0 is chosen in this way to ensure both sides of (4) have the same dimension. It can be seen that the slope of lifetime curve increases considerably from 50 Hz to 1500 Hz. This indicates a lower lifetime for OIP samples that are exposed to higher frequency stress. Table II shows the parameters of lifetime curves for the two target frequencies. For 50 Hz parameters are very sensitive and even small change of the medians along each electric field stress could influence n and k considerably. In general, to have more reliable parameters we need to do experiments at lower electric field level and with time to breakdown much longer than what we have presented here.

TABLE II. PARAMETERS OF LIFETIME CURVE SHOWN IN FIG. 5

Parameter	n	k
One layer 50 Hz	25,64	5×10^{46}
One layer 1500 Hz	7.15	7×10^{12}

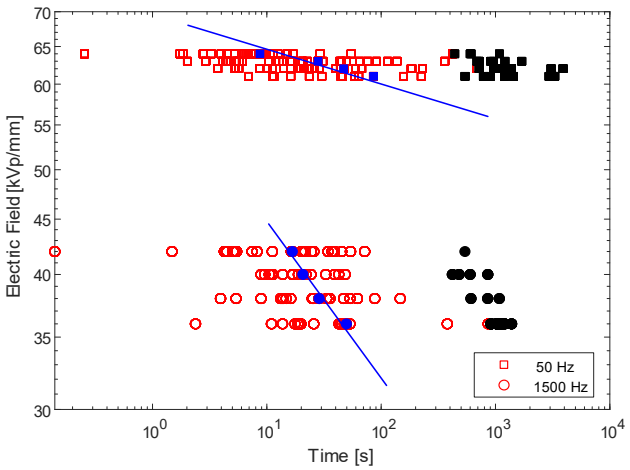

Fig. 5. Lifetime curves for one layer of OIP at 50 Hz and 1500 Hz. Black dots represent the halted experiments. n is equal to 7.15 for 1500 Hz and 25.64 for 50 Hz.

It was also observed that through the whole experiments (for both ramp sinusoidal and step sinusoidal tests) breakdown could happen at both polarities, most of them take place close to the peak of voltage waveform (both polarities) and sometimes off the peak. Examples of such breakdown that happen off the peak are shown in Fig. 6.

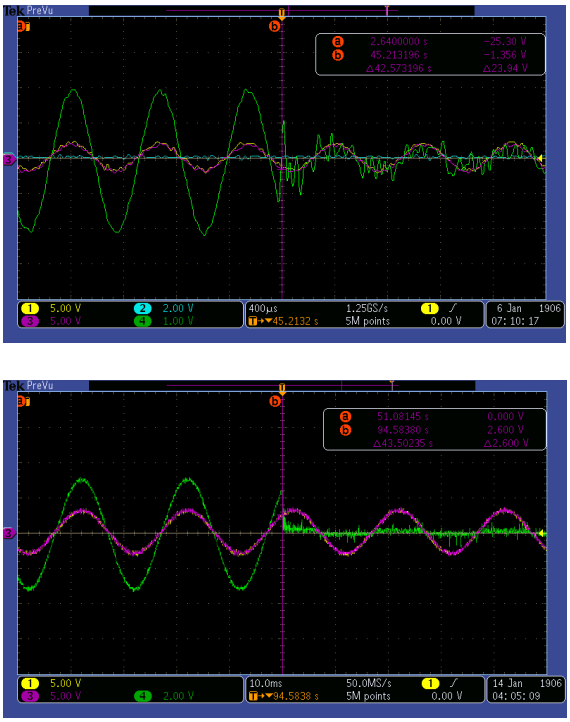

Fig. 6. Breakdown moment at different polarities and different phase of the sinusoidal waveform. Top: example of 1500 Hz, bottom: example of 50 Hz

V. Conclusion

In this study, breakdown strength and lifetime of OIP samples were investigated at 50 Hz and 1500 Hz. For the ramp sinusoidal test, it could be concluded that breakdown strength is lower and at the same time more spread at 1500 Hz compared with 50 Hz. To obtain lifetime curves, step sinusoidal voltage waveform was used. It was found that the slope of lifetime curve for 1500 Hz is much lower than that at 50 Hz. This indicates that for a desired lifetime, the permissible electric field at 1500 Hz must be much lower than at 50 Hz, which means more insulation material for a given design is required at 1500 Hz.

The future plan is to extend this work and perform similar experiments at higher frequency range (2kHz-30 kHz). This will help the readers to have better understanding of OIP aging exposed to high frequency high voltage stress, which can also provide indication for the selection of the suitable insulation material for MFT.

Acknowledgment

The project is funded by Dutch TKI Urban Energy program which is greatly acknowledged.

References

[1] Moonesan, Mohammad Saleh, et al. “Time to Failure of Medium-Voltage Form-Wound Machine Turn Insulation Stressed by Unipolar Square Waves.” IEEE Transactions on Dielectrics and Electrical Insulation, vol. 22, no. 6, IEEE, Dec. 2015, pp. 3118–25, doi:10.1109/TDEI.2015.005201.

[2] Peng Wang, et al. “The Influence of Repetitive Square Wave Voltage Parameters on Enameled Wire Endurance.” IEEE Transactions on Dielectrics and Electrical Insulation, vol. 21, no. 3, IEEE, June 2014, pp. 1276–84, doi:10.1109/TDEI.2014.6832275.

[3] Weijun Yin. “Failure Mechanism of Winding Insulations in Inverter-Fed Motors.” IEEE Electrical Insulation Magazine, vol. 13, no. 6, Nov. 1997, pp. 18–23, doi:10.1109/57.637150.

[4] Hammarström, TJ Å., et al. "Partial discharges in motor wires at PWM voltages of different smoothness." Proceedings of 2014 International Symposium on Electrical Insulating Materials. IEEE, 2014.

[5] Peng Wang, et al. “The Influence of Repetitive Square Wave Voltage Rise Time on Partial Discharge Inception Voltage.” 2016 IEEE Conference on Electrical Insulation and Dielectric Phenomena (CEIDP), vol. 2016-Decem, IEEE, 2016, pp. 759–62, doi:10.1109/CEIDP.2016.7785635.

[6] [54] Grzybowski, S., E. A. Feilat, and P. Knight. "Accelerated aging tests on magnet wires under high frequency pulsating voltage and high temperature." 1999 Annual Report Conference on Electrical Insulation and Dielectric Phenomena (Cat. No. 99CH36319). Vol. 2. IEEE, 1999.

[7] Cavallini, Andrea, et al. “Power Electronics and Electrical Insulation Systems - Part 2: Life Modeling for Insulation Design.” IEEE Electrical Insulation Magazine, vol. 26, no. 4, IEEE, July 2010, pp. 33–39, doi:10.1109/MEI.2010.5511187.

[8] Konig, D., N. Hardt, and V. Scherb. "Comparitive insulation tests with DC and AC at 50 Hz and 50 kHz." 1998 Annual Report Conference on Electrical Insulation and Dielectric Phenomena (Cat. No. 98CH36257). Vol. 2. IEEE, 1998.

[9] MG Niasar, RC Kiiza, N Taylor, H Edin, “Effect of partial discharges on thermal breakdown of oil - impregnated paper”, EEJ Transactions on Electrical and Electronic Engineering, Volume 10, Pages S14-S18, 2015.

[10] Jiayang Wu, Huifei Jin, Armando Rodrigo Mor and Johan Smit, “The Effect Of Frequency On The Dielectric Breakdown Of Insulation Materials In HV Cable Systems”, in proceedings of ISEIM 2017.

[11] D. Fabiani, G. C. Montanari, A. Cavallini and G. Mazzanti, "Relation between space charge accumulation and partial discharge activity in enameled wires under PWM-like voltage waveforms," in IEEE Transactions on Dielectrics and Electrical Insulation, vol. 11, no. 3, pp. 393-405, June 2004.

[12] Yikun Zhao, Guoqiang Zhang, Kang Li, Yang Liu and Fuyao Yang, “A Test Standard for Winding Insulation and Air Gaps of Dry-Type HV-HF Transformer”, 22nd International Conference on Electrical Machines and Systems (ICEMS), 2019.

[13] M Ghaffarian Niasar, Nathaniel Taylor, Patrick Janus, Xiaolei Wang, Hans Edin, R Clemence Kiiza, “Partial discharges in a cavity embedded in oil-impregnated paper: effect of electrical and thermal aging”, IEEE Transactions on Dielectrics and Electrical Insulation, Volume 22, Issue 2, Pages 1071-1079, 2015.